Geologie en Mijnbouw **76:** 121–134, 1997.

Late Cenozoic magnetostratigraphy (11 – 0 Ma) of the Dongshanding and Wangjiashan sections in the Longzhong Basin, western China

Ji-Jun Li[1], Xiao-Min Fang[1,2], Rob Van der Voo[2], Jun-Jie Zhu[1], Conall Mac Niocaill[2], Ji-Xiu Cao[1], Wei Zhong[1], Huai-Lu Chen[1], Jianli Wang[1], Jian-Ming Wang[1] & Yie-Chun Zhang[1]
[1] *Department of Geography, Lanzhou University, Lanzhou, Gansu 730 000, China;* [2] *Department of Geological Sciences, the University of Michigan, Ann Arbor, MI 48109-1063, U.S.A.*

Received 30 August 1996; accepted in revised form 30 July 1997

Key words: reversals, Miocene, Pliocene

Abstract

A paleomagnetic study of the 510-m-thick Wangjiashan section of Late Miocene and Pliocene terrestrial sediments reveals a fairly complete reversal record with ages from 11 to 1.8 Ma. The magnetostratigraphy of the Dongshanding section, located nearby, reveals a partially overlapping reversal record with ages from 2.2 to 0 Ma, and facilitates correlation of the Wangjiashan section with the global polarity time scale. A new stratigraphic division of the Wangjiashan section replaces the name Linxia formation by five new formation names, based on lithologic variation and mammalian fossil finds. The new formations and their magnetostratigraphically determined ages are: Dongshan Formation (c. 1.75–2.6 Ma), Jishi Fm. (c. 2.6–3.6 Ma), Hewangjia Fm. (4.5–6.0 Ma), Liushu Fm. (6.0–7.6 Ma), and Dongxiang Fm. (7.6–c. 12 Ma). The Neogene stratigraphy and fossil mammals suggest that the nearby part of the Tibetan Plateau experienced a persistent denudation during the Late Miocene and Early Pliocene, but that it was uplifted more rapidly at about 3.6 Ma.

Introduction

Magnetostratigraphy of land-based Neogene deposits has received increased attention in the last decade, especially owing to the efforts of the Fort Hoofddijk paleomagnetic group in Utrecht (e.g. Langereis et al. 1984, Zijderveld et al. 1986, 1991, Hilgen 1991a, b, Van Hoof et al. 1993, Krijgsman et al. 1994a, b, 1995, 1996, Hilgen et al. 1995, Garcés et al. 1996). Because of this, we are pleased to dedicate this paper to Hans Zijderveld, who tirelessly promoted and stimulated this area of research.

Late Cenozoic sedimentary sequences are widely distributed in western China, including the Tibetan Plateau (Wang 1990). In general, they can be divided into three major types: light-colored fluviolacustrine or aeolian sediments, conglomerates, and red beds (de Chardin 1936, Li 1984, Yin et al. 1988). Paleontologic data have shown that the light-colored sediments were deposited during the Late Pliocene and Quaternary, the conglomerates in the Plio-Pleistocene, and the red beds mainly in the Tertiary (Chiu et al. 1979, Li 1984, Wang 1990, Qiu & Qiu 1995). This stratigraphy may reflect uplift of the nearby part of the Tibetan Plateau and climatic changes related to it (Li et al. 1979, Yin et al. 1988), especially where the conglomerate beds are concerned (Li et al. 1979, Liu et al. 1996), because of their widespread appearance at about 3.5 Ma all along the northern and northeastern margin of the Plateau. However, uncertainties about the rates and magnitude of neotectonic processes have led to controversies about the phasing of uplift of the Plateau (Fort 1996 and references therein). These ambiguities are in need of resolution, especially if we are to solve issues related to global climate change or to improve numerical models of climate prediction (Kutzbach et al. 1989, Ruddiman & Kutzbach 1989). The general lack of knowledge about precise ages in western China hampers stratigraphic correlation. Therefore, the Chinese government has launched a national project (1993–2010) aimed at unraveling the Tibetan Plateau history and its impact on regional and global change.

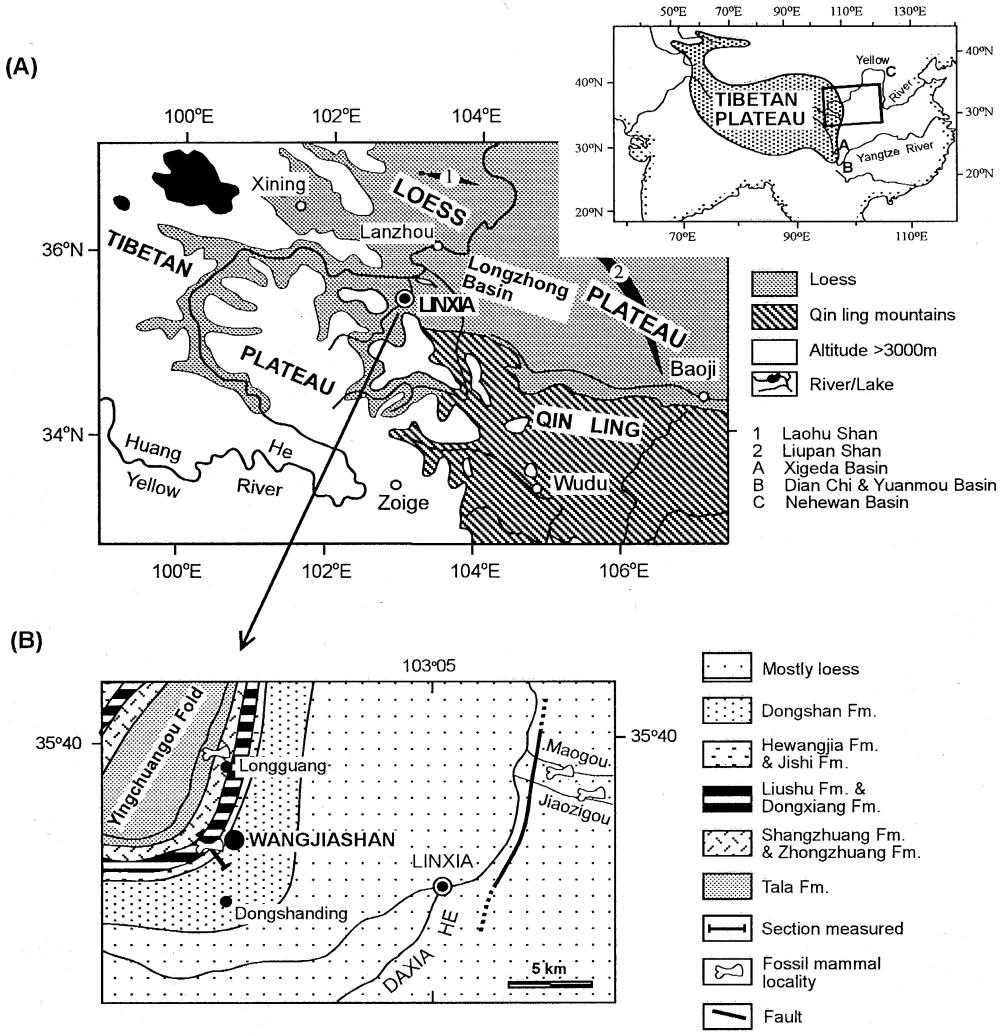

Figure 1. Location maps of the Longzhong Basin (A) and the Dongshanding and Wangjiashan sections (B). The location of other basins, which developed during the Pliocene, is shown in the inset.

Here we present our first magnetostratigraphic results from the Longzhong Basin obtained through a cooperation between the universities of Lanzhou and Michigan, and funded by this national project of the People's Republic of China.

Geologic setting and stratigraphy

The Longzhong Basin is one of the largest Tertiary basins in China. Located in central Gansu Province and eastern Qinghai Province, it is bordered by the Tibetan Plateau to the southwest, by the Qin Ling mountains to the south (Figure 1A) and by the lower-elevation ranges of the Laohu Shan and Liupan Shan to the north and east (Figure 1). The large Longzhong Basin can be divided into sub-basins, such as the Linxia, Lanzhou and Xining basins, which contain several hundred to up to 2000 m of Tertiary red beds. Mainly fluviolacustrine in origin, these beds form the base of the Loess Plateau (Young & Bien 1937, Gansu Regional Geological Survey Team (GRGST) 1965, 1984, Liu 1985). Ages suggested for the red beds range from possibly Eocene to Pliocene, on the basis of fossil mammals (GRGST 1965, 1984, Li & Qiu 1980, Qiu et al. 1987, 1990, Xie 1991, 1996, Gu et al. 1992, 1995a, b), but are in need of refinement. We have first focussed our work

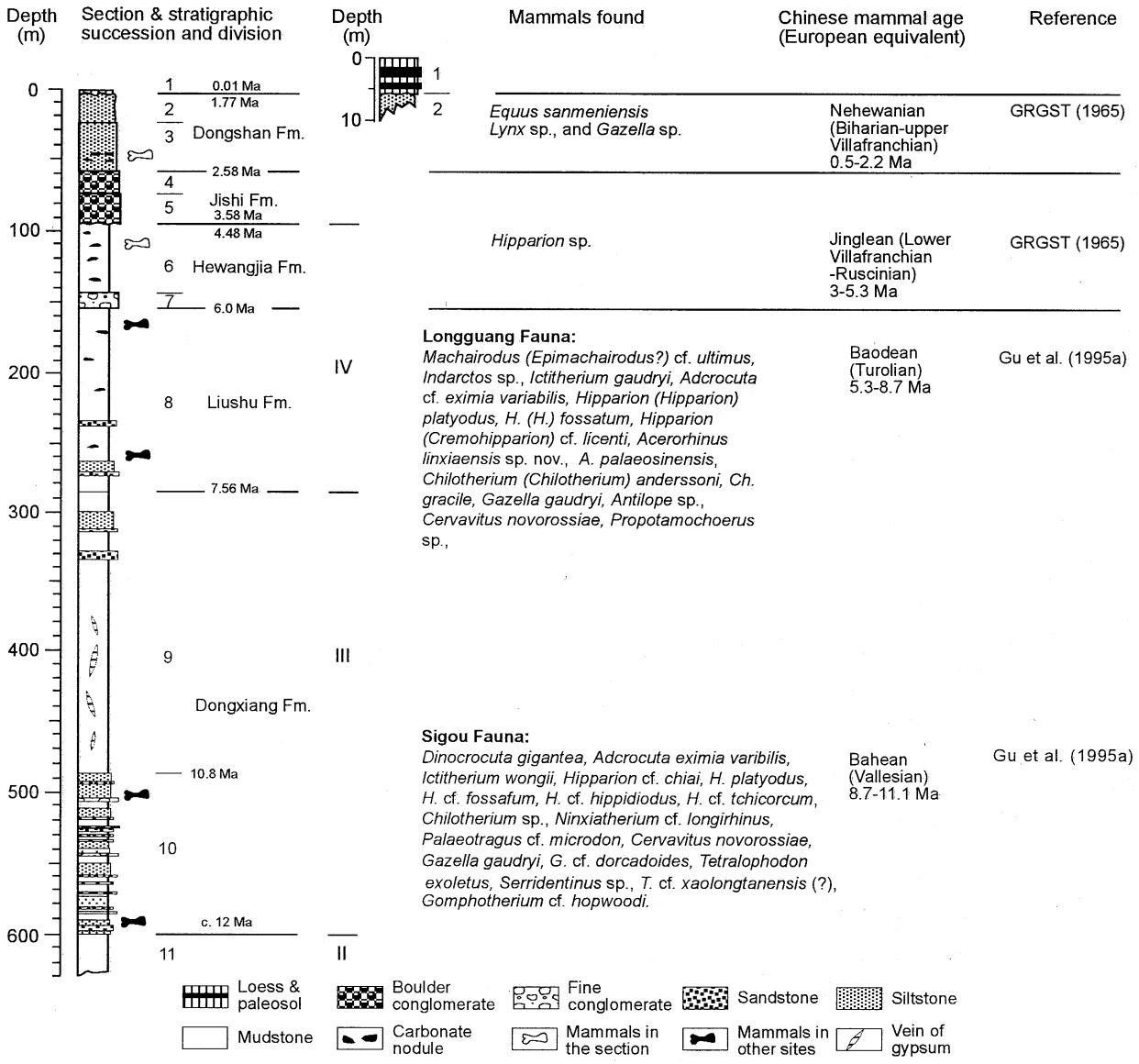

Figure 2. Lithology, lithostratigraphic units (1–11), new formation names with approximate ages determined in this study, lithologic units (II-IV) of GRGST (1965), and fossil occurrences for the Wangjiashan section (location in Figure 1B).

on the Linxia Basin, because of its nearly continuous stratigraphy and its vicinity to the Tibetan Plateau.

The Linxia Basin is divided into a western and an eastern part by a normal NNE-striking fault parallel to the river Daxia He (Figure 1B), which is a tributary of Huang He (the Yellow River). The western basin has been a tectonically active depocenter, infilled by more than 1600 m of red beds, followed by 30 to 60 m of distinctive boulder conglomerates and up to several hundred meters of Late Pliocene and Quaternary light-colored (greenish-gray) lacustrine sediments and (yellowish) loess (GRGST 1965, 1984). West of Linxia, where we sampled the Wangjiashan section, the beds are strongly folded (Figure 1B). In contrast, the eastern basin is relatively less deep, being tectonically more stable and infilled by only 400 to 800 m of red beds and Quaternary loess.

The red beds were first studied by the Gansu Regional Geological Survey Team (GRGST 1965). They divided the red beds into four lithologic units (I to

IV from old to young) and named the entire section the Linxia Formation. A fossil mammal (*Hipparion*) was found in the youngest lithologic unit IV of the Wangjiashan section, a type section for the Linxia Formation (Figure 2), which at the time suggested a Pliocene age (GRGST 1965). In the absence of other fossils, the entire red-bed sequence in the Linxia Basin was thought to be of this age (GRGST 1965). Subsequently, many other researchers have used this Pliocene age as representative of similar red-bed sequences in western China (e.g. Li 1984). Only recently, when Miocene fossil mammals were discovered in the lower part of the red beds (lithologic units II–IV), were the strata re-assigned to older epochs (Qiu et al. 1987, 1990, Gu et al. 1995a, b).

The upper 510 m of the Wangjiashan type section were measured and sampled in a northwesterly direction across the southeastern limb of the Yingchuangou Anticline (Figure 1B). We divided it into eleven lithostratigraphic units that are labeled consecutively from young to old in Figure 2. *Unit 1* consists of up to 6 m of loess and paleosols in two parallel sections. Nearby, e.g. on an ancient river terrace at Dongshanding (Figure 1) to the south of Wangjiashan, the loesses and paleosols are up to 60 m thick.

Units 2 and 3 (depths 2–59 m), are herein called the Dongshan Formation (Fm.). This formation contains a lower 33 m of light-brownish-yellow shallow-lacustrine siltstones in which many carbonate nodules are embedded, and 24 m of greenish-gray deeper-water siltstones on top. The Plio-Pleistocene fossil mammals *Equus sanmeniensis*, *Lynx* sp. and *Gazella* sp. were found in unit 3 (GRGST 1965, see also Lindsay et al. 1980).

Units 4 and 5 are named the Jishi Fm., and contain 35-m-thick conglomerates with cobbles of up to 15 cm in diameter. Elsewhere, units 4 and 5 are up to 60 m thick, with cobbles up to 2 m in size. The cobbles are subrounded, are weakly cemented together, and display imbricated textures in the upper part (59–77 m). The cobbles are mainly sandstones, but quartz and granite clasts are found as well, apparently derived from Carboniferous and Triassic sandstones and granites in the Tibetan Plateau to the southwest of the Linxia Basin. Unit 4 reveals bedding interfaces with cobbles showing imbrications that face southwest to south, indicating these to be their provenance directions. In the lower part (unit 5, 77–94 m) the cobbles have subrounded to subangular shapes, are strongly carbonate-cemented, and show weakly imbricated to massive textures. Unit 4 has the appearance of high-energy fluvial deposits, whereas unit 5 with its weak bedding, weak imbrications and cobbles mixed with sand and mud appears to consist of alluvial and debris flows.

Units 6 and 7 are named the Hewangjia Fm. The upper unit (94–143 m) is a yellowish-brown shallow-lacustrine mudstone with many carbonate nodules, 2 to 5 cm in size. The lower member (unit 7, 143–154 m) contains carbonate-cemented fluvial conglomerates that are rich in fine subrounded to subangular pebbles, mainly 1 to 2 cm in diameter.

The Liushu Fm. (*unit 8*, 154–286 m) consists of brown mudstones with carbonate nodules, interbedded with a few thin grayish marl layers in the middle part and a minor siltstone-sandstone layer near the bottom. This siltstone-sandstone layer is interpreted as a lakeshore or delta deposit. At two different depths in the same formation at Longguang village, about 8 km north of the Wangjiashan section, a large variety of fossil mammals has been excavated and is called the Longguang Fauna (listed in Figure 2). This fauna indicates a Late Miocene age for the Liushu Fm. (Gu et al. 1995a), at the locations marked by black bones in Figure 2.

Units 9 and 10 are called the Dongxiang Fm. Unit 9 (286–486 m) is one of the more distinct sequences in the basin, with 200 m of purple shallow-lacustrine mudstone, intercalated with somewhat cyclic 0.5 to 1 m thick white and gray-greenish marl layers, that form stripes that resemble those of a zebra. The sequence contains many large veins of secondary gypsum (Figure 2). Unit 10 (486–600 m) consists of 114 m of cyclic graded beds of conglomerates, siltstones and mudstones, interpreted as delta and lacustrine deposits, respectively. The pebbles of the gravels are subrounded to subangular and have diameters of 1 to 3 cm. Only the uppermost 24 m of these graded beds were sampled. In unit 10 at Sigou in Guanghe County, about 30 km east of the Wangjiashan section, the Sigou mammal fauna was discovered (listed in Figure 2), with a late Middle Miocene age (Gu et al. 1995a). The approximate stratigraphic levels of this fauna are marked by the black bones in the lower Dongxiang Fm. in Figure 2.

Bedding attitudes vary from the southeast to the northwest, towards the core of the Yingchuangou Anticline (Figure 1B), from 65°/16° to 123°/76° (dip direction/dip). The stratigraphy appears to be continuous except at the depths of 2 and 94 m, where unconformities exist between the loess and the Dongshan Fm. and between the Jishi and Hewangjia Fms, respectively (Figure 2).

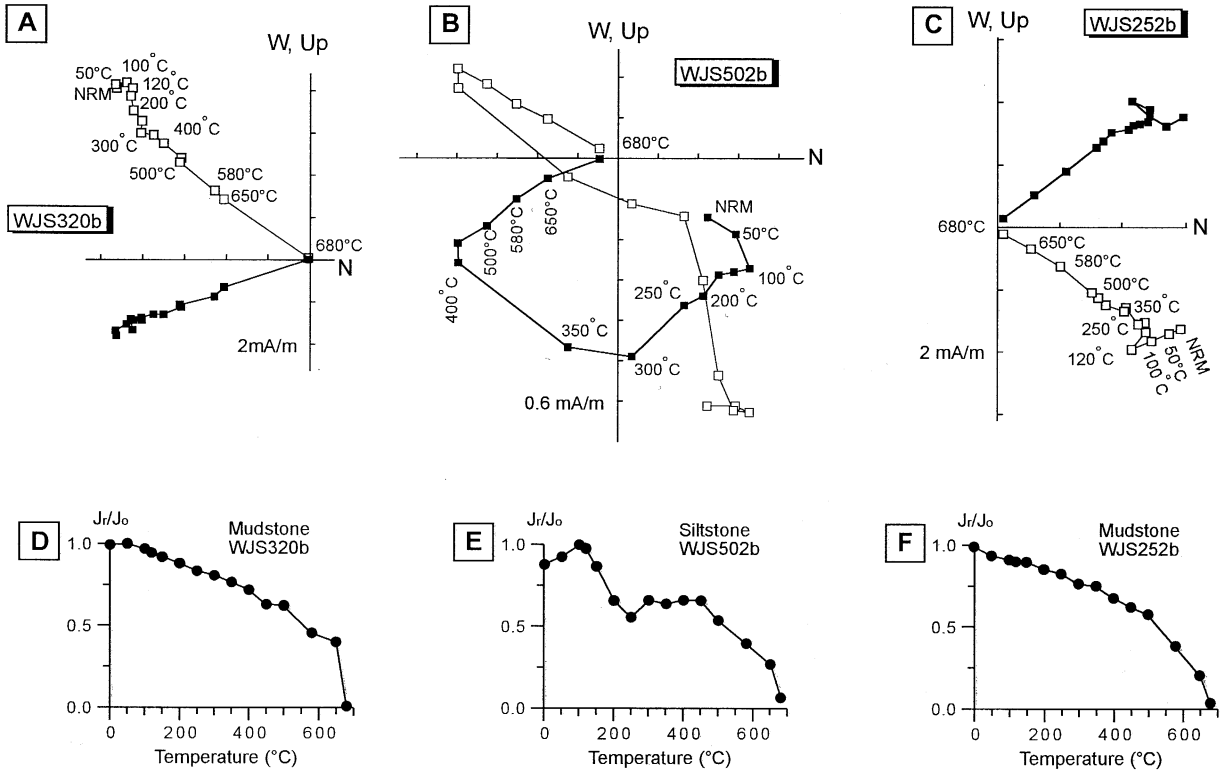

Figure 3. Thermal demagnetization diagrams (A–C) of three representative samples, in tilt-corrected coordinates, with sample numbers corresponding to depths in the Wangjiashan section. Full (open) symbols represent projections onto the horizontal (vertical) plane. D–F illustrate the change in intensity during thermal demagnetization of the same samples as in A–C.

Sampling and laboratory work

To facilitate sampling of fresh material, a 1-m-deep trench was dug along the entire length of the Wangjiashan section. Samples were taken at 0.5 to 1-m stratigraphic intervals in the upper 59 m, and at 2-m intervals in the lower 451 m. Exceptions were made for the conglomerates where sampling intervals depended on the availability of finer-grained lenses. At each site, one large oriented block was collected from which three cubic sub-samples of $2 \times 2 \times 2$ cm^3 were taken. At a later date, additional sub-samples were taken for those levels (sites) where confirmation of the magnetostratigraphy seemed important. A total of 915 sub-samples were measured in the laboratories.

The natural remanent magnetization (NRM) of one set of sub-samples was measured with a Digico magnetometer at Lanzhou University, and stepwise alternating field (AF) demagnetization was employed in twelve steps of 5 mT up to peak fields of 60 mT. Progressive thermal demagnetization in fifteen steps (varying between 10 and 50°C) up to 680°C was carried out for the other two sets of sub-samples as well as for the supplemental samples. The magnetization behavior during thermal demagnetization was measured with a Schonstedt SSM-2 magnetometer at the Chengdu Institute of Geology (for the upper 150 m of section) and with a 2G cryogenic magnetometer in a magnetically shielded room at the University of Michigan (for the lower 360 m of section and for the supplemental samples).

Representative thermal demagnetization diagrams (Figure 3) show that there are up to three lower-blocking-temperature components superimposed as overprints on a higher-temperature characteristic magnetization (e.g. Figure 3B). The overprints generally are randomly oriented for the lowest blocking-temperature intervals and have northerly and downward directions in intermediate intervals (e.g. Figure 3B, 300–400°C). Above 450°C, however, all overprints appear to have been removed and characteristic magnetizations appear to be isolated with clear normal or reversed directions (Figures 3A–C). Most samples show a distributed decay in remanent intensity below 650°C, whereupon the magnetization decays rapidly

up to 680°C (e.g. Figure 3D), indicating that hematite is the major magnetic carrier in these red beds.

Paleomagnetic directions were obtained from principal-component analysis of the demagnetization patterns in each sample. The directions obtained in AF demagnetization are generally similar to those of the thermal demagnetizations, but differ to some extent for the purple mudstones of the Dongxiang Fm., where isolation of components is better in thermal demagnetization. Where AF demagnetization of the hematite-bearing beds suggested imperfectly cleaned directions, only the directions obtained in thermal demagnetization were used to calculate site-mean directions. Mean directions for most other sites were obtained by averaging the three or four sub-sample directions at each level.

Site-mean directions were used to calculate virtual geomagnetic pole (VGP) positions, and the latitudes of these VGPs were used to plot a reversal stratigraphy without correcting for the deviations of the mean directions from the present-day field direction as these deviations are small for the Neogene.

Magnetostratigraphy of the Dongshanding section

In order to substantiate the correlation of the Wangjiashan section to the geomagnetic polarity time scale of Cande & Kent (1995), we briefly discuss the magnetostratigraphic results of an overlapping section located on a river terrace at Dongshanding (Figures 1B, 4). Results for the Quaternary part of this section are published elsewhere (Li et al. 1997) and show a complete reversal record in the upper 78 m of the section. The N1/R1 magnetozone boundary in this section is correlated with the Brunhes/Matuyama boundary, N2 with the Jaramillo subchron, N3 with the Cobb Mountain subchron and N4 with the Gilsa event. Various ^{14}C and thermoluminescence age determinations for the loesses and paleosols (S0–S23) of this section support these correlations (Li et al. 1997).

Before the loesses and paleosols began to accumulate on the terrace, the Yellow River deposited a thick conglomerate unit, the Jinggoutou Fm., on top of the lacustrine Dongshan Fm.. The Jinggoutou Fm. reveals reversed-polarity (R4) directions assigned to the Matuyama chron at about 1.66–1.75 Ma. The top of the Dongshan Fm. shows the base of this R4 reversed interval.

New results from the main part of the Dongshan Fm. (78 to 150 m depth in Figure 4) reveal four normal (N5 to N8) and four reversed-polarity (R5 to R8) intervals, with the N5 and N6 normal magnetozones interpreted to represent the Olduvai subchron; this correlation is supported by amino-acid-racemization (AAR) dating carried out at the Tianjin Institute of Geology, which yielded an age of about 1.77 Ma for trees and about 1.83 Ma for ostracodes. N7 and N8 can then be correlated to the two Reunion subchrons in the lower Matuyama chron. The Jishi Fm. did not contain suitable rock types for sampling in the Dongshanding section, but the top of the underlying Hewangjia Fm. shows normal polarity (N9), in agreement with results from the Wangjiashan section, to be discussed below.

The main part of the Dongshan Fm., if it is correctly interpreted as representing the Olduvai subchron, reveals a high sedimentation rate in the Dongshanding section. We will see below that the same is found for the Wangjiashan section, where ages are constrained to be < 2.2 Ma by fossils (Figure 2). The ages of the fossils and AAR dates that are all younger than 2.2 Ma make it highly unlikely that we have misidentified a Gauss Normal polarity record (older than 2.55 Ma) in the sections.

Magnetostratigraphy of the Neogene formations of the Wangjiashan section

The samples of this section were measured in two stages, with the upper 140 m being demagnetized mostly by AF, whereas the 147–510 m interval was treated later with mostly thermal demagnetization.

Below the Holocene loess-paleosol on top, the upper 120 m of section yielded eight normal zones N1–N8 and eight reversed zones R1–R8 (Figure 5). Zones N1–N3 and R1–R3 are observed in the siltstones of the Dongshan Fm. This formation is here truncated at the top, but is continuous in the Dongshanding section, where the uppermost part of the Dongshan Fm. is reversed (R4 in Figure 4). The major part of the formation records normal polarities (N6) which are correlated to the Olduvai subchron. Hence, we assume that in the Wangjiashan section N1 can also be correlated with the Olduvai subchron, and N2 and N3 with the two Reunion events (Figure 5).

We calculate an average deposition rate of 4.35 cm/ka from the interval between the base of the Olduvai subchron at 1.95 Ma and the bottom of the Reunion at 2.27 Ma. Extrapolating at a constant rate, the base of the Dongshan Fm. is calculated to be about

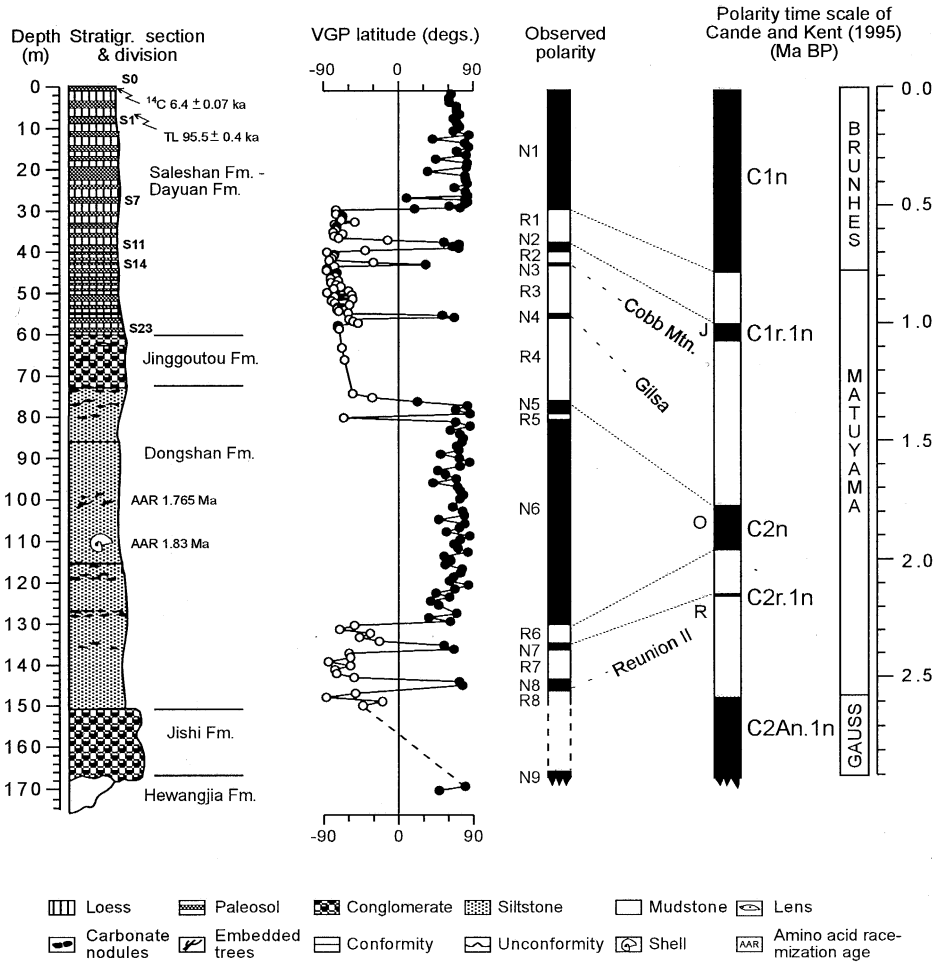

Figure 4. Stratigraphic column, virtual geomagnetic pole (VGP) latitudes, and observed polarities of the Dongshanding section (for location see Figure 1), correlated with the geomagnetic polarity time scale of Cande & Kent (1995). Solid (open) symbols represent VGPs in the northern (southern) hemisphere. J = Jaramillo, O = Olduvai, and R = Reunion subchron. AAR = amino-acid-racemization ages; S0 to S23 are paleosols.

2.58 Ma, whereas the top of the formation is about 1.84 Ma (Table 1).

As a consequence of the assignment of R3 to the base of the Matuyama chron, N4–N6 in the Jishi Fm. most likely correspond to the Gauss normal chron. Using the timescale of Cande & Kent (1995), R4 at a depth of 74.5 m and R5 at a depth of 84 m correlate to the Kaena (3.04–3.11) and Mammoth (3.22–3.33) subchrons, respectively (Figure 5). Extrapolating at a constant sedimentation rate during the deposition of the Jishi Fm. of 3.65 cm/ka, its top and bottom are estimated to be about 2.6 Ma and 3.6 Ma (Table 1).

Between the Jishi Fm. and the underlying Hewangjia Fm., a major unconformity is observed in the field, so that magnetic reversals in the Hewangjia Fm. are not necessarily consecutive with those in the Jishi Fm. However, the Longguang Fauna of Late Miocene age, found in the upper part of the Liushu Fm. (Figure 2), constrains the age of the immediately overlying Hewangjia Fm. Fossil mammals found in the Liushu Fm. at other localities also have suggested that it belongs to the Baodean (= Turolian) stage (Xie 1996). Our preferred correlation of R6–R7 in the Hewangjia Fm. is to the middle part of the Gilbert chron, with N7 and N8 correlating to the Sidufjall and Thvera subchrons. This implies that the Cochiti normal subchron and the upper part of the Gilbert chron are missing from the section, being truncated by the unconformity, and that N6 consists of two non-consecutive parts (N6A and N6B in Figure 5). Alternative correlations (e.g. N7 =? Cochiti, N8 =? Nunivak) are less likely, as they would require a hiatus in the lower Hewangjia Fm.,

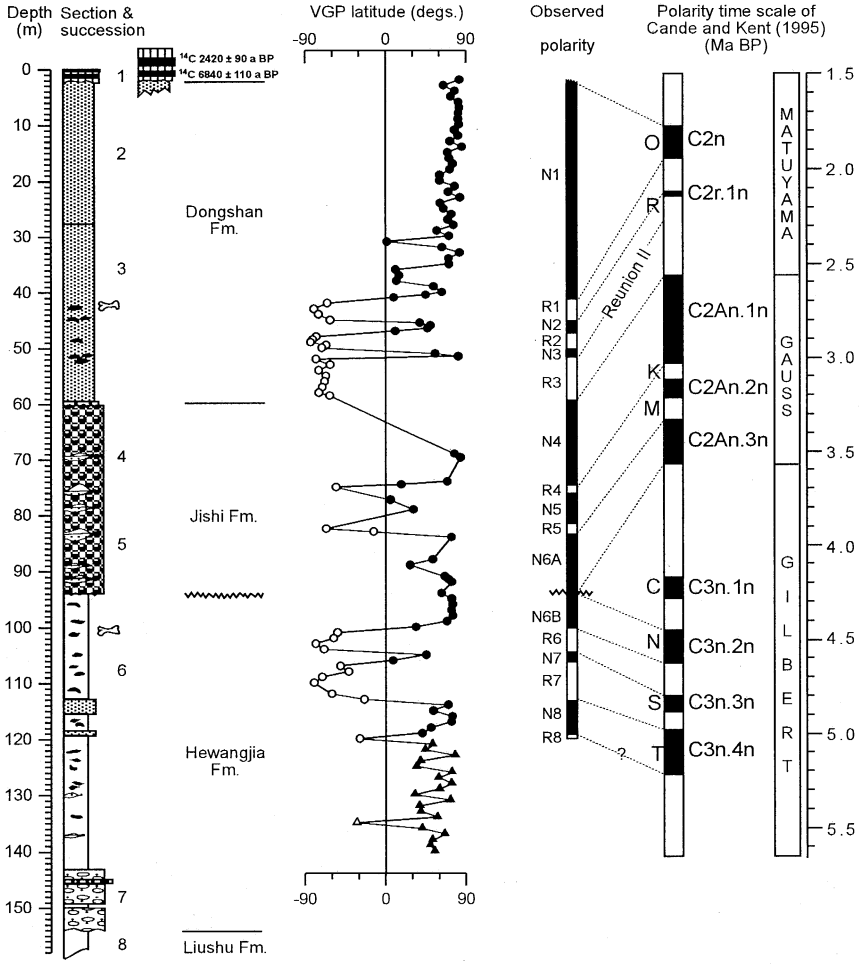

Figure 5. Stratigraphic column, virtual geomagnetic pole (VGP) latitudes, and observed polarities of the upper 150 m of the Wangjiashan section, correlated with the geomagnetic polarity time scale (Cande & Kent 1995). O = Olduvai, R = Reunion, K = Kaena, M = Mammoth, C = Cochiti, N = Nunivak, S = Sidufjall and T = Thvera subchron. Lithologic legend as in Figure 4. Triangles at depths of 121–140 m represent directions that are suspected to be mostly secondary.

with the lower Gilbert reversed magnetozone missing (or very condensed?) in our record, for which there is no evidence.

The top of N6B is estimated to be about at the top of the Nunivak event based on an upwards extrapolated sedimentation rate (3.61 cm/ka, using Cande & Kent 1995) that is calculated between the bottom of the Nunivak, and the top of the Thvera subchron (Table 1). Therefore, the hiatus represented by the unconformity can be estimated to span the interval of about 3.6 to 4.5 Ma.

There is no significant lithologic change between 113 and 143 m, but the normal-polarity directions below R8 appear to be anomalous, in the sense that they cannot be made to match the geomagnetic polarity time scale (GPTS); these directions are plotted in Figure 5 as triangles. Except for a reversal (R8) at 120 m and another one at 136 m, where one thermally demagnetized sample shows a reversed direction, we observe a long continuous normal-polarity interval, which does not correlate with the GPTS. Results in preparation for the Maogou section, about 18 km ENE of Wangjiashan (Figure 1B), have shown a short N8-equivalent interval (interpreted as the Thvera subchron) and a long R8-equivalent reversed record, interpreted as the lower Gilbert chron, in this part of the Hewangjia Fm. We suspect that our trench has not uncovered sufficiently fresh material in this part of the Wangjiashan section and that the normal-polarity magnetic directions below R8 are caused by secondary overprints.

Table 1. Ages of the interpreted chrons and stratigraphic boundaries in the Wangjiashan section.

Depth (m)	Stratigraphic or reversal boundary	Polarity chron Cande & Kent (1995)	Age (Ma)
2	Top of Dongshan Fm.	C2n	~1.84
41.5	Bottom of Olduvai	C2n	1.95
45.5	Top of Reunion I	C2r.1n	2.14
51.5	Bottom of Reunion II		2.27
59	Bottom of Dongshan Fm.	C2An.1n	2.581
59	Top of Jishi Fm.	C2An.1n	2.581
74	Top of Kaena	C2An.2n	3.04
84	Bottom of Mammoth	C2An.3n	3.33
94	Bottom of Jishi Fm.	C2An.3n	~3.58
94	Nunivak/Top of Hewangjia Fm.	C3n.2n	4.48
100.5	Bottom of Nunivak	C3n.2n	4.62
104.5	Top of Sidufjall	C3n.3n	4.8
106.5	Bottom of Sidufjall	C3n.3n	4.89
113.5	Top of Thvera	C3n.4n	4.98
120.5	Bottom of Thvera	C3n.4n	5.23
148		C3An.1n	>5.894
154	Bottom of Hewangjia Fm. /Top of Liushu Fm.		~6
169		C3An.1n	6.137
197		C3An.2n	6.269
215		C3An.2n	6.567
245		C3Bn	6.935
253		C3Bn	7.091
255		C3Br.1n	7.135
257		C3Br.1n	7.17
273		C4n.1n	7.432
286	Bottom of Lishu Fm. /Top of Dongxiang Fm.		7.562
291		C4n.2n	7.65
309		C4n.2n	8.072
333		C4An	8.699
349		C4An	9.025
369.5		C4Ar.1n	9.23
383		C4Ar.1n	9.308
398.5		C4Ar.2n	9.58
403.5		C4Ar.2n	9.642
410.5		C5n	9.74
486	Bottom of upper member of Dongxiang Fm.		~10.8
497		C5n	10.949
503		C5r.1n	11.052
508		C5r.1n	11.099

In the lower 360 m of the section, the Liushu and Dongxiang Fms. reveal 15 normal zones N1–N15 and 15 reversed zones (Figure 6). The Late and late Middle Miocene ages suggested for this part of the section by the Longguang and Sigou faunas (Figure 2), roughly correlate with the Turolian (5.3–8.7 Ma) and Vallesian (8.7–11.1 Ma) stages of European land mammals (Garcés et al. 1996; Krijgsman et al. 1996). Vein gyp-

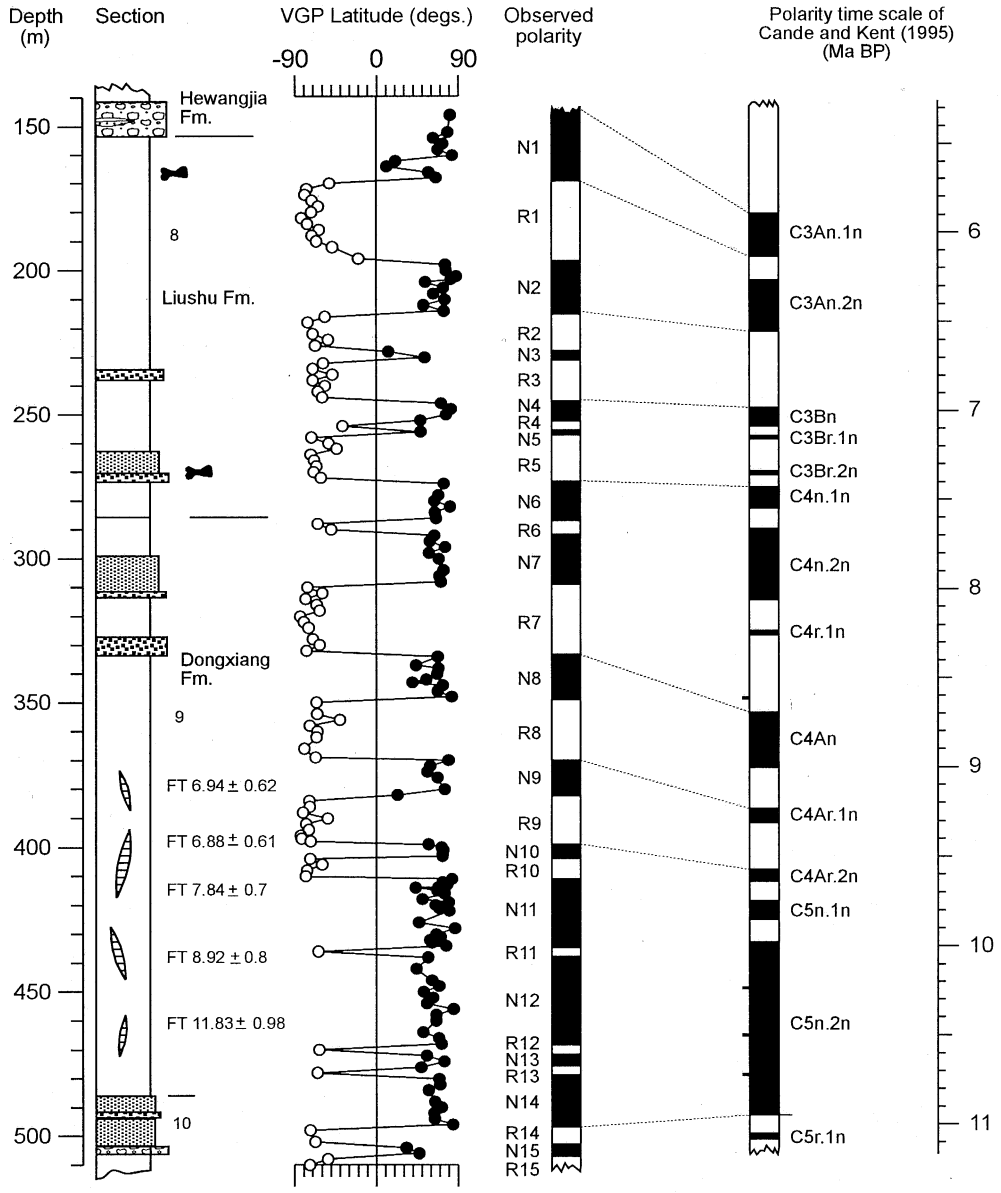

Figure 6. Stratigraphic column, virtual geomagnetic pole (VGP) latitudes, and observed polarities of the lower 360 m of the Wangjiashan section, correlated with the geomagnetic polarity time scale (Cande & Kent 1995). Cryptochrons in chron 5 are represented by tickmarks on the left of the column. Lithologic legend as in Figure 4. FT indicates fission-track ages of gypsum veins (in Ma).

sum crystals in the middle Dongxiang Fm. (357–470 m in depth; Figure 2) have yielded fission-track (FT) ages (Chen et al. 1995) of about 7–12 Ma (Figure 6). The gypsum is secondary in origin and must have formed later than the deposits in which it occurs. Although there are large errors associated with the FT dates, and considering arguments about the reliability of FT dates from minerals forming at low temperatures (Wagner 1992, Carter et al. 1995), these dates provide a rough estimate of this part of the stratigraphy, which implies that the Dongxiang Fm. formed at about 7–12 Ma, in agreement with the ages provided by the mammals.

N1 and N2 can be correlated with the two normal zones, 3An.1n and 3An.2n, of Cande & Kent (1995). Bracketing the Wangjiashan section at the base, a long predominantly normal-polarity interval is found

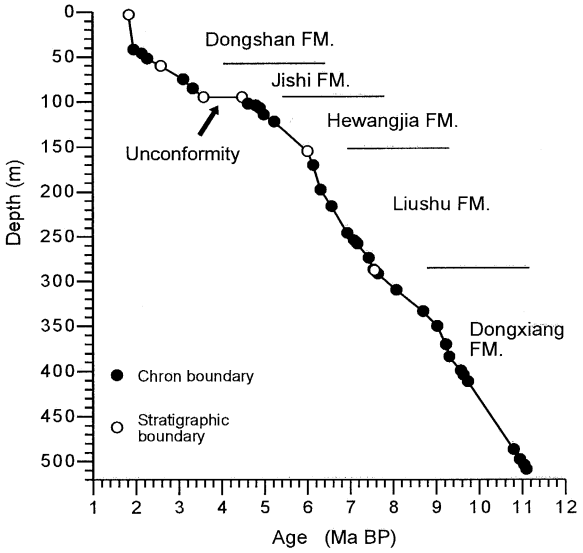

Figure 7. Depth versus age plot of the observed magnetozones of the Wangjiashan section (see Table 1) and their ages based on the geomagnetic polarity time scale of Cande & Kent (1995).

at depths of 410 to 490 m that correlates well with chron 5n. In between chrons 3An and 5n, we observe most of the subchrons of the GPTS, and we correlate these as shown in Figure 6 (see also Table 1).

N3 does not correspond to any zones in the GPTS of Cande & Kent (1995), but R11, R12 and R13 have corresponding representations in the three cryptochrons in chron 5n (short ticks in Figure 6). It is noteworthy that Garcés et al. (1996) have also found these three reverse magnetozones in the Vallesian of the Les Fonts locality in Spain. We have not observed the short subchrons 3Br.2n, 4r.1n and 5n.1r.

On the basis of these correlations, the Liushu Fm. can be estimated as having been deposited from 7.6 to 6 Ma. The upper lithostratigraphic unit of the Dongxiang Fm. formed from 10.8 to 7.6 Ma, and the bottom of the measured Wangjiashan section formed at c. 11.1 Ma (Figure 6). The base of the Dongxian Fm. is constrained in age by the Sigou fauna and can be estimated as about 12 Ma by extrapolation of the sedimentation rate.

Figure 7 illustrates the age–depth relationships of the interpreted magnetic zones and the formation boundaries. A nearly linear relationship can be observed for the magnetic zones and these boundaries, with the major exception occurring at the unconformity at the base of the Jishi conglomerates. By extrapolating the linear age–depth relationships for the Hewangjia, Liushu, and upper Dongxiang formations, the base of the entire red-bed sequence, with its 1600 m of thickness, is estimated to be about 30 Ma or Late Oligocene in age. Preliminary and unpublished magnetostratigraphy of the Maogou section confirms this age through identification of chron C10.

Discussion

The magnetostratigraphic dating of the upper 510 m of the Wangjiashan section demonstrates that it spans the interval of about 11–1.8 Ma. The base of the entire Tertiary section is estimated at about 30 Ma, which is much older than the Pliocene age previously considered (GRGST 1965, Li 1984). Hence, the previous name, Linxia formation, can no longer be seen as suitable to describe the red beds in the Linxia Basin. The variation in lithology within the red beds has allowed us to propose five new formation names for the measured part of the section in this paper (Figure 2).

We will discuss only a few highlights of the stratigraphic section and their implications for the environmental conditions and the neotectonics of the area. The yellowish-brown mudstones of the Liushu Fm. (unit 8) mark an end to the purplish-red sediments of the Dongxiang Fm., indicating a change in the sedimentary environment at about 7.55 Ma. This may correlate with a large global climate change inferred for about 6.5–8 Ma ago from continental as well as deep-sea sedimentary records (Loutit & Keigwin 1982, Quade et al. 1989, Morgan et al. 1994, Quade & Cerling 1995).

Lithostratigraphic unit 7 contains a conglomerate bed of about 5.6 Ma to 6 Ma, but it is of much less prominence than the Jishi conglomerates of lithostratigraphic units 4 and 5, which were deposited between 3.6 and 2.6 Ma. The latter conglomerates likely indicate a large tectonosedimentary change, as their thickness can be over 60 m, with boulders larger than 1–2 m in diameter in some parts of the area. It appears that everywhere in western China, yellowish-brown and red mudstone sequences are truncated by coarse conglomerates with uncertain ages (de Chardin 1936, GRGST 1984, Liu et al. 1996). Hence, the age of the Jishi conglomerates is significant for its relationship to neotectonics.

Lithostratigraphic units 2 and 3 consist of siltstones with greenish-gray to yellowish colors that suggest a reducing environment of deposition. At Dongshanding many fresh or somewhat decayed trees (mainly pines) are embedded in lithostratigraphic unit 2 of latest Pliocene–earliest Pleistocene age (c. 2–1.7 Ma). We

infer a moist and reduced sedimentary environment, in contrast to the earlier Neogene oxidizing environment during the deposition of the brown and red mudstones. At the time of this transition, the Yellow River drainage system started to form in the Longzhong Basin, replacing the Linxia lake environment of earlier Pliocene time (Li et al. 1997).

From these environmental conditions a few inferences may be made about the uplift of the nearby Tibetan Plateau. At the base of the oldest lithostratigraphic sequence studied (unit 10), graded beds with fine conglomerates, sandstones, siltstones and mudstones suggest persistent but mild tectonic uplift and denudation of the Tibetan Plateau. The overlying thick mudstones (lithostratigraphic units 9–6) imply that the elevation caused by this mild uplift was reduced to a lowland due to long-term (10–4 Ma) weathering, forming a so-called trans-drainage peneplain or planation surface (Selby 1985). This peneplain may now have become a main surface of the Plateau (Li et al. 1979, Shackleton & Chang 1988). During this long denudation, the fluviolacustrine mudstone deposits continued without much variation, except for the fine conglomerate bed of lithostratigraphic unit 7 at about 6 Ma.

We do not recognize in our sedimentary sequence the full-scale uplift of the Himalayas and/or Tibetan Plateau inferred for about 7–8 Ma (Quade et al. 1989, Harrison et al. 1992), but it may well be that the northeastern part of the Plateau, adjacent to the Longzhong Basin, was uplifted at a later time. A global climate change, rather than a local Asian monsoon event, has also been inferred for this time (Loutit & Keigwin 1982, Cerling et al. 1993, Morgan et al. 1994).

The nature of the fossil mammals with ages of c. 4–10 Ma has suggested an environment characterized by forests and steppe in a relatively hot lowland resembling the African savanna (Gu et al. 1995a, b). They closely resemble the fauna found in the southern foothills of the Himalayas (Barry et al. 1982, 1985, Flynn et al. 1995). This has been interpreted (e.g. Li et al. 1979) to mean that before the Early Pliocene, large mammals were able to migrate freely across the Tibetan Plateau, suggesting that its elevation was much less than today's. However, others (e.g. Fort 1996) have disputed this argument.

Whatever the case may be, at about 3.6 Ma the deposition of the Jishi boulder conglomerates is indicative of a pronounced uplift of the portion of the Tibetan Plateau adjacent to the Linxia Basin, as well as farther west. All along the northern margin of the Plateau, thick boulder conglomerates appear roughly at this time as suggested by fossil mammals and some paleomagnetic data (Huang et al. 1993, Li 1984, Qiu & Qiu 1995, Liu et al. 1996). Simultaneously, many large down-faulted basins formed around the Plateau (Figure 1), e.g. the Xigeda Basin at the eastern margin of the Plateau, which formed at 3.29 Ma (Qian et al. 1984), the Dian Chi and Yuanmou Basin at the southeastern margin that formed at 3.4 to 3.9 Ma (Yian & Bai 1988, Qian & Zhou 1991), and the Nihewan Basin in north China that formed at 3.2 Ma (Chen et al. 1978). It appears that the northern and northeastern part of the Tibetan Plateau was uplifted rapidly at about 3.6 Ma. After this strong uplift phase, sedimentation rates remained high for a major part of the Dongshan Fm., as indicated by the thick interval representing the Olduvai subchron. However, besides uplift of a Tibetan source area, this may indicate also that the Asian monsoon system was strengthened as suggested by the moist environment inferred from the Dongshan Fm. (which was deposited in a deeper-water lake than earlier mudstones), pollen data (Pan et al. 1995), sedimentary geochemistry (Xi et al. 1996), and the onset of deposition of the Chinese loess (Liu 1985).

Acknowledgements

We thank Miguel Garcés and Wout Krijgsman for thorough and helpful reviews. This work was supported by the Chinese National Project on Studies on Formation and Evolution of the Qinghai-Xizang Plateau, Environmental Change and Ecological System; and the National Science Foundation of China.

References

Barry, J.C., E.H. Lindsay & J.L. Jacobs 1982 A biostratigraphic zonation of the Middle and Upper Siwaliks of the Potwar Plateau of northern Pakistan – Palaeogeogr. Palaeoclimat. Palaeoecol. 37: 95–130

Barry, J.C., N.M. Johnson & S.M. Raza 1985 Neogene mammalian faunal change in southern Asia: Correlations with climatic, tectonic, and eustatic events – Geology 13: 637–644

Cande, S.C. & D.V. Kent 1995 Revised calibration of the geomagnetic polarity timescale for the Late Cretaceous and Cenozoic – J. Geophys. Res. 100: 6093–6095

Carter, A., C.S. Bristow & A.J. Hurford 1995 The application of fission track analysis to the dating of barren sequences; examples from red beds in Scotland and Thailand – Geol. Soc. London Spec. Publ. 89: 57–68

Cerling, T. E., Y. Wang & J. Quade 1993 Expansion of C4 ecosystems as an indicator of global ecological change in late Miocene – Nature 361: 344–345

Chen, G.L., J.L. Lin & S.L. Li et al. 1978 A preliminary paleomagnetic study of the Nihewan strata – Geol. Sci. 3: 247–252 (in Chinese, with English abstract)

Chen, H.L., X.M. Fang, J.J. Li & S.C. Kang 1995 Fission-track dating of the gypsum in the Linxia Basin and its age. In: Scientific Commision of the National Project on the Tibetan Plateau (eds.) Study on the Formation and Evolution of the Qinghai-Xizang Plateau, Environmental Change and Ecological System – Sci. Press, Beijing: 73–76 (in Chinese with English abstract)

Chiu, C.S., C. Li & C. Chiu 1979 The Chinese Neogene–a preliminary review of the mammalian localities and faunas – Ann. Géol. Pays. Hellén., h.s., 1: 263–272

de Chardin, P.T. 1936 Notes on Continental Geology – Bull. Geol. Soc. China 16: 195–220

Flynn, L.J., J.C. Barry, M.E. Morgan, D. Pilbeam, L.L. Jacobs & E.H. Lindsay 1995 Neogene Siwalik mammalian lineages: Species longevities, rates of change, and modes of speciation – Palaeogeogr. Palaeoclimat. Palaeoecol. 115: 249–264

Fort, M. 1996 Late Cenozoic environmental changes and uplift on the northern side of the central Himalaya: a reappraisal from field data – Palaeogeogr. Palaeoclimat. Palaeoecol. 120: 123–145

Gansu Regional Geological Survey Team (GRGST) 1965 Introduction to the 1: 200,000 Geological Map of the People's Republic of China: sheet Linxia – Lanzhou. 42 pp (in Chinese)

Gansu Regional Geological Survey Team (GRGST) 1984 Tertiary System of Gansu – Gansu Geology 2: 1–40 (in Chinese with English abstract)

Garcés, M., J. Agustí, L. Cabrera & J.M. Parés 1996 Magnetostratigraphy of the Vallesian (late Miocene) in the Vallès-Penedès basin (NE Spain) – Earth Planet. Sci. Lett. 142: 381–396

Gu, Z.G., S.H. Bai, X.T. Zhang, Y.Z. Ma, S.H. Wang & B.Y. Li 1992 Division and correlation of the Neogene in the Guide and Huailong basins, Qinghai Province – J. Stratigr. 16: 96–104, 119 (in Chinese)

Gu, Z.G., S.H. Wang, S.Y. Hu & D.T. Wei 1995a Research progress on biostratigraphy of Tertiary Red Beds in Linxia Basin, Gansu Province. In: Scientific Commision of the National Project on the Tibetan Plateau (eds.) Study on the Formation and Evolution of the Qinghai-Xizang Plateau, Environmental Change and Ecological System – Sci. Press, Beijing: 91–95 (in Chinese with English abstract)

Gu, Z.G., S.H. Wang, S.Y. Hu & D.T. Wei 1995b Discovery of *Giraffokeryx* in China and the Tertiary chronostratigraphy of Linxia, Gansu Province – Chin. Sci. Bull. 40: 758–760

Harrison, T.M., D. Copeland, W.S.F. Kidd & A. Yin 1992 Raising Tibet – Science 255: 1663–1670

Hilgen, F.J. 1991a Astronomical calibration of Gauss to Matuyama sapropels in the Mediterranean and implication for the Geomagnetic Polarity Time Scale – Earth Planet. Sci. Lett. 104: 226–244

Hilgen, F.J. 1991b Extension of the astronomically calibrated (polarity) time scale to the Miocene/Pliocene boundary – Earth Planet. Sci. Lett. 107: 349–368

Hilgen, F.J., W. Krijgsman, C.G. Langereis, L.J. Lourens, A. Santarelli & W.J. Zachariasse 1995 Extending the astronomical (polarity) timescale into the Miocene – Earth Planet. Sci. Lett. 136: 495–510

Huang H.F., Z.L. Peng, W. Lu & J.J. Zheng 1993 Paleomagnetic division and comparison of the Tertiary system in Jiuxi and Jiudong Basins – Acta Geologica Gansu 2: 6–16 (in Chinese with English abstract)

Krijgsman, W., F.J. Hilgen, C.G. Langereis & W.J. Zachariasse 1994a The age of the Tortonian/Messinian boundary – Earth Planet. Sci. Lett. 121: 533–547

Krijgsman, W., C.G. Langereis, R. Daams & A.J. Van der Meulen 1994b Magnetostratigraphic dating of the middle Miocene climate change in the continental deposits of the Aragonian type area in the Calatayud-Teruel basin (Central Spain) – Earth Planet. Sci. Lett. 128: 513–526

Krijgsman, W., F.J. Hilgen, C.G. Langereis, A. Santarelli & W.J. Zachariasse 1995 Late Miocene magnetostratigraphy, biostratigraphy and cyclostratigraphy from the Mediterranean – Earth Planet. Sci. Lett. 136: 475–494

Krijgsman, W., M. Garcés, C.G. Langereis, R. Daams, J. Van Dam, A.J. Van der Meulen, J. Agustí & L. Cabrera 1996 A new chronology for the middle to late Miocene continental record in Spain – Earth Planet. Sci. Lett. 142: 367–380

Kutzbach, J. E., P.J. Guetter, W.F. Ruddiman & W.L. Prell 1989 Sensitivity of climate to late Cenozoic uplift in Southern Asia and the American West: Numerical experiments – J. Geophys. Res. 94: 18393–18407

Langereis, C.G., W.J. Zachariasse & J.D.A. Zijderveld 1984 Late Miocene magnetobiostratigraphy of Crete – Mar. Micropaleontol. 8: 261–281

Li, C.K. & Z.X. Qiu 1980 Early Miocene mammalian fossils of Xining Basin, Qinghai – Vertebrata Palasiatica 18: 210–218 (in Chinese, with English abstract)

Li, J.J., S.X. Wen, Q.S. Zhang, F.B. Wang, B.X. Zhang & B.Y. Li 1979 A discussion on the period, amplitude and type of the uplift of the Qinghai-Xizang Plateau – Scientia Sinica 22: 1314–1328

Li, J.J., X.M. Fang, R. Van der Voo, J.J. Zhu, C. Mac Niocaill, Y. Ono, B.T. Pan, W. Zhong, J.L. Wang, T. Sasaki, Y.T. Zhang, J.X. Cao, S.C. Kang & J.M. Wang 1997 Magnetostratigraphic dating of river terraces: rapid and intermittent incision by the Yellow River of the northeastern margin of the Tibetan Plateau during the Quaternary – J. Geophys. Res. 102: 10121–10132

Li, Y.T. (ed.) 1984 Tertiary of China – Sci. Press, Beijing, 251 pp

Lindsay, E.H., N.D. Opdyke & N.M. Johnson 1980 Pliocene dispersal of the horse *Equus* and late Cenozoic mammalian dispersal events – Nature 287: 135–138

Liu, T.S. (ed.) 1985 Loess and the Environment – China Ocean Press, Beijing, 251 pp

Liu, T.S., D. Menglin & E. Derbyshire 1996 Gravel deposits on the margins of the Qinghai-Xizang Plateau, and their environmental significance – Palaeogeogr. Palaeoclimat. Palaeoecol. 120: 159–170

Loutit, T.S., L.D. Keigwin Jr 1982 Stable isotopic evidence for latest Miocene sea-level fall in the Mediterranean region – Nature 300: 163–166

Morgan, M.E., J.D. Kingston & B.D. Marino 1994 Carbon isotopic evidence for the emergence of C4 plants in the Neogene from Pakistan and Kenya – Nature 367: 162–165

Pan, A.D., J.J. Li & X.M. Fang 1995 A preliminary study of the Quaternary pollen record in the Dongshanding section in Linxia and its environmental implications. In: J. J. Li (ed.) Paper collections of the 1995 Annual meeting on the National Tibetan Project (in Chinese), Lanzhou University: 30–37

Qian, F. & X.G. Zhou 1991 Quaternary Geology and Palaeoanthropology of Yuanmou, Yuanmou, China – Sci. Press, Beijing: 1–60

Qian, F., S.J. Xu, F.B. Chen & Y.T. Zhao 1984 Study on the paleomagnetism of the Xigeda Formation – Mountain Res. 2: 275–282 (in Chinese, with English abstract)

Qiu, Z.X. & Z.D. Qiu 1995 Chronological sequence and subdivision of Chinese Neogene mammalian faunas – Palaeogeogr. Palaeoclimat. Palaeoecol. 116: 41–70

Qiu, Z.X., J.Y. Xie & D.F. Yan 1987 The new discovery of *Chilotherium* in Hezheng County of Gansu Province, China – Scientia Sinica (B) 5: 545–552 (in Chinese)

Qiu, Z.X., H.Y. Xie & D.F. Yan 1990 Discovery of some early Miocene mammalian fossils from Dongxiang, Gansu – Vertebrata Palasiatica 28: 9–24 (in Chinese with English abstract)

Quade, J. & T.E. Cerling 1995 Expansion of C4 grasses in the late Miocene of N. Pakistan: evidence from stable isotopes in paleosols – Palaeogeogr. Palaeoclimat. Palaeoecol. 115: 91–116

Quade, J., T.E. Cerling & J.R. Bowman 1989 Development of Asian monsoon revealed by marked ecological shift during the latest Miocene in northern Pakistan – Nature 342: 163–166

Ruddiman, W.F., & J.E. Kutzbach 1989 Forcing of late Cenozoic Northern Hemisphere climate by plateau uplift in Southern Asia and the American West – J. Geophys. Res. 94: 18409–18427

Selby, M.J. 1985 Earth's Changing Surface: An Introduction to Geomorphology – Clarendon Press, Oxford, 607 pp

Shackleton, R.M. & C.F. Chang 1988 Cenozoic uplift and deformation of the Tibetan Plateau: the geomorphological evidence – Phil. Trans. R. Soc. Lond. A 327: 365–377

Van Hoof, A.A.M., B.J. Van Os, J.G. Rademakers, C.G. Langereis & G.J. De Lange 1993 A paleomagnetic and geochemical record of the upper Cochiti reversal and two subsequent precessional cycles from southern Sicily (Italy) – Earth Planet. Sci. Lett. 117: 235–250

Wagner, G.A. 1992 Fission Track Dating – Kluwer, Dordrecht, 152 pp

Wang, P.X. 1990 Neogene stratigraphy and paleoenvironments of China – Palaeogeogr. Palaeoclimat. Palaeoecol. 77: 315–334

Xi, X.X., D.F. Mu, X.M. Fang & J.J. Li 1996 Variation of Cl^- content in paleo-Dongshan Lake during Early Pleistocene and monsoonal evolution – J. Glaciol. Geocryol. 18: 125–130

Xie, J.Y. 1991 Neogene stratigraphy and fossil mammals of Gansu – J. Stratigr. 15: 35–41 (in Chinese)

Xie, J.Y. 1996 A compilation of Neogene fossil mammals of Gansu – J. Lanzhou Univ. (Series B) 32: 235–237

Yian, Q.T. & S.G. Bai 1988 Cenozoic in the Kunming basin. In: Pu, Q.Y. (ed.) Contribution to the Quaternary Glaciology and Quaternary Geology 5 – Geol. Publ. House, Beijing: 252–261 (in Chinese)

Yin, J.X., J. T. Xu, C.J. Liu & H. Li 1988 The Tibetan plateau: regional stratigraphic context and previous work – Phil. Trans. R. Soc. Lond. A 327: 5–52

Young, C.C. & J. Bien 1937 Cenozoic geology of the Kaolan-Yungteng area of central Kansu – Bull. Geol. Soc. China 16: 221–260

Zijderveld, J.D.A., W.J. Zachariasse, P.J.J.M. Verhallen & F.J. Hilgen 1986 The age of the Miocene-Pliocene boundary – Newsl. Stratigr. 16: 169–181

Zijderveld, J.D.A., F.J. Hilgen, C.G. Langereis, P.J.J.M. Verhallen & W.J. Zachariasse 1991 – Integrated magnetostratigraphy and biostratigraphy of the upper Pliocene-lower Pleistocene from the Monte Singa and Crotone areas in Calabria, Italy – Earth Planet. Sci. Lett. 107: 697–714